Two- and four-quasiparticle states in the interacting boson model: Strong-coupling and decoupled band patterns in the SU(3) limit

Vretenar, Dario; Paar, Vladimir; Bonsignori, G.; Savoia, M.

Source / Izvornik: **Physical Review C - Nuclear Physics, 1990, 42, 993 - 1003**

Journal article, Published version
Rad u časopisu, Objavljena verzija rada (izdavačev PDF)

https://doi.org/10.1103/PhysRevC.42.993

Permanent link / Trajna poveznica: https://urn.nsk.hr/urn:nbn:hr:217:158238

Rights / Prava: In copyright / Zaštićeno autorskim pravom.

Download date / Datum preuzimanja: **2024-07-11**

Repository / Repozitorij:

Repository of the Faculty of Science - University of Zagreb

Two- and four-quasiparticle states in the interacting boson model: Strong-coupling and decoupled band patterns in the SU(3) limit

D. Vretenar and V. Paar
Prirodoslovno-matematički Fakultet, University of Zagreb, 41000 Zagreb, Yugoslavia

G. Bonsignori and M. Savoia
Istituto Nazionale di Fisica Nucleare, Sezione of Bologna and Department of Physics "A. Righi", Via Irnerio 46, Bologna, Italy
(Received 25 January 1990)

An extension of the interacting boson approximation model is proposed by allowing for two- and four-quasiparticle excitations out of the boson space. The formation of band patterns based on two- and four-quasiparticle states is investigated in the SU(3) limit of the model. For hole-type (particle-type) fermions coupled to the SU(3) prolate (oblate) core, it is shown that the algebraic K-representation basis, which is the analog of the strong-coupling basis of the geometrical model, provides an appropriate description of the low-lying two-quasiparticle bands. In the case of particle-type (hole-type) fermions coupled to the SU(3) prolate (oblate) core, a new algebraic decoupling basis is derived that is equivalent in the geometrical limit to Stephens' rotation-aligned basis. Comparing the wave functions that are obtained by diagonalization of the model Hamiltonian to the decoupling basis, several low-lying two-quasiparticle bands are identified. The effects of an interaction that conserves only the total nucleon number, mixing states with different number of fermions, are investigated in both the strong-coupling and decoupling limits. All calculations are performed for an SU(3) boson core and the $h\frac{11}{2}$ fermion orbital.

I. INTRODUCTION

The interacting boson approximation (IBA) model[1] in its various versions has been remarkably successful in the description of a variety of nuclear structure phenomena. The approach based on the IBA model was also extended to the description of two-quasiparticle high-spin states in even-even nuclei.[2-5] The purpose of this paper is to extend the IBA-1 model by allowing for two- and four-quasiparticle excitations out of the boson space. In Sec. II we give a short outline of the model. As one of the possible applications, we consider the description of rotational bands based on two- and four-quasiparticle states in deformed even-even nuclei. All calculations are performed for the illustrative case: a prolate boson core characterized by SU(3) symmetry and the fermion space restricted to the unique parity orbital $h\frac{11}{2}$. In Sec. III we consider the case of hole-type (particle-type) fermions coupled to the SU(3) prolate (oblate) core. It is shown that the lowest two-quasiparticle bands near the yrast line can be described by the algebraic K-representation basis that is the analog of the strong-coupling basis of the geometrical model. With the inclusion of an interaction that conserves only the total nucleon number, mixing states with different number of fermions, we obtain a crossing of the ground-state band with the lowest two-quasiparticle band.

In Sec. IV we investigate the formation of band patterns for the case of particle-type (hole-type) fermions coupled to the SU(3) prolate (oblate) core. For the lowest two-quasiparticle high-spin states the boson-fermion interaction is repulsive and the bands are decoupled. For the description of these bands we derive a new algebraic basis that, for large boson number, becomes equivalent to the strong-coupling–to–rotation-aligned transformation of Stephens. In both the strong-coupling and decoupling limits we study the behavior of the moment of inertia as a function of angular velocity.

II. OUTLINE OF THE MODEL

In the simplest version of the interacting boson approximation model, referred to as IBM-1,[1] a system of N bosons of angular momentum 0 (s bosons) and 2 (d bosons) interacts with one- and two-body forces. A standard microscopic interpretation of the IBM is that the s and d bosons are approximations to valence nucleon pairs. The fact that the bosons in the IBM-1 can be regarded as collective fermion pair states introduces a natural link between the IBM-1 and the shell model. Most directly, this link is established through the introduction of the generalized seniority scheme.[1] Another possible interpretation of the IBM-1 is given by the truncated quadrupole phonon model. Then the destruction of an s boson and the creation of a d boson corresponds to the excitation of a quadrupole phonon. The connection between the two possible microscopic interpretations of the IBM-1 has been reviewed, for example, in Ref. 6.

In its basic versions (IBM-1 and IBM-2), the interacting boson model has been applied mostly in the description of low-spin states in medium heavy and heavy nuclei. On the other hand, a large amount of data on high-spin states in these regions have been accumulated in the last decade. In order to attempt a description of high-spin

 ©1990 The American Physical Society

states, various extensions of the IBM have been investigated that include selective noncollective two-fermion states in addition to s and d bosons. In this paper we introduce an extension of the IBM-1 by including two- and four-fermion noncollective states. It is assumed that a boson can break to form a noncollective fermion pair. This means that an even-even nucleus with $2N$ valence nucleons is described in the Hilbert space

$$\mathcal{H} \rightarrow |N \text{ bosons}\rangle \oplus |(N-1) \text{ bosons} \otimes 1 \text{ broken pair}\rangle \oplus |(N-2) \text{ bosons} \otimes 2 \text{ broken pairs}\rangle \ .$$

Such an extension should allow the description of high-spin states well above the second backbending, as well as a more realistic description of low-spin states.

The fermions in broken pairs will occupy the same set of valence orbitals from which the bosons are constructed. However, for the description of the yrast region the most important orbitals occupied by noncollective fermion pairs will be the unique parity high-j orbitals as, for example, $h_{\frac{11}{2}}$ or $i_{\frac{13}{2}}$. In the following we employ the truncated quadrupole phonon version of the IBM-1. In this representation the one and two broken pairs are represented by two- and four-quasiparticle states, and we require that

$$n_{\rm qp} + 2n_B \leq 2N \ ,$$

where $n_{\rm qp}$ and n_B denote the number of quasiparticles and quadrupole phonons in the basis states, respectively. We use the Hamiltonian

$$H = H_B + H_F + H_{BF} \ , \tag{1}$$

where H_B is the IBM-1 boson Hamiltonian[1] expressed in the TQM form.[7] H_F denotes the fermion Hamiltonian for identical quasiparticles

$$H_F = \sum_{\alpha} E_\alpha a^\dagger_\alpha \tilde{a}_\alpha + \tfrac{1}{4} \sum_{\substack{ab \\ cd}} \sum_{JM} V^J_{abcd} A^\dagger_{JM}(ab) A_{JM}(cd) \ . \tag{2}$$

The notation for single-quasiparticle states is

$$\alpha \equiv (n_a, l_a, j_a, m_a) \equiv (a, m_a) \ ,$$

and the quasiparticle-pair operator is defined as

$$A^\dagger_{JM}(ab) = [A_{JM}(ab)]^\dagger = \sum_{m_a m_b} \langle j_a m_a j_b m_b | JM \rangle a^\dagger_\beta a^\dagger_\alpha \ , \tag{3}$$

$$V^J_{abcd} = (u_a u_b u_c u_d + v_a v_b v_c v_d) G(abcdJ) + 4 v_a u_b v_c u_d F(abcdJ) \ , \tag{4}$$

where the matrix elements G and F of a two-nucleon interaction in the coupled basis are defined in Ref. 8.

The boson-fermion interaction H_{BF} contains dynamical and exchange terms as used in the interacting boson-fermion model;[9]

$$H_{BF} = H_{\rm dyn} + H_{\rm exc} \ . \tag{5}$$

In the particle-truncated quadrupole phonon (PTQM) representation of the IBFM,[10] the dynamical part that conserves the number of fermions is given by

$$H_{\rm dyn} = Q^F_2 \cdot Q^B_2 \ , \tag{6}$$

where the boson and fermion quadrupole operators are, respectively,

$$Q^B_{2\mu} = b^\dagger_{2\mu} (N - \hat{N})^{1/2} + (N - \hat{N})^{1/2} \tilde{b}_{2\mu} + \chi (b^\dagger_2 \tilde{b}_2)_{2\mu} \ , \tag{7}$$

$$Q^F_{2\mu} = \Gamma_0 \sum_{j_1 j_2} (u_{j_1} u_{j_2} - v_{j_1} v_{j_2}) \langle j_1 \| r^2 Y_2 \| j_2 \rangle (a^\dagger_{j_1} \tilde{a}_{j_2})_{2\mu} \ . \tag{8}$$

The exchange term reads

$$H_{\rm exc} = \sum_{j_1 j_2 j_3} \Lambda_{j_1 j_2 j_3} : \{ (a^\dagger_{j_1} \tilde{b}_2)_{j_3} (\tilde{a}_{j_2} b^\dagger_2)_{j_3} \}_0 : \ , \tag{9}$$

where

$$\Lambda_{j_1 j_2 j_3} = -\Lambda_0 2\sqrt{5/(2j_3+1)} (u_{j_1} v_{j_3} + v_{j_1} u_{j_3}) \times (u_{j_2} v_{j_3} + v_{j_2} u_{j_3}) \langle j_3 \| r^2 Y_2 \| j_1 \rangle \langle j_3 \| r^2 Y_2 \| j_2 \rangle \ . \tag{10}$$

An additional term in the boson-fermion interaction that conserves only the total nucleon number, mixing states with different number of fermions, is defined as

$$H_{\rm mix} = A^F_2 \cdot \tilde{b}_2 + \text{H.c.} \ , \tag{11}$$

where

$$A^F_{2\mu} = -\frac{\varepsilon_0}{2} \sum_{j_1 j_2} \langle j_1 \| r^2 Y_2 \| j_2 \rangle (u_{j_1} v_{j_2} + u_{j_2} v_{j_1}) (a^\dagger_{j_1} a^\dagger_{j_2})_{2\mu} \ . \tag{12}$$

The total boson-fermion interaction is then

$$H_{BF} = H_{\rm dyn} + H_{\rm exc} + H_{\rm mix} \ . \tag{13}$$

The Hamiltonian (1) is diagonalized in a model space consisting of states with N bosons, $N-1$ bosons plus two fermions, and $N-2$ bosons plus four fermions:

$$\begin{aligned} &|n\nu I\rangle, \quad (n \leq N) \\ &|(j_1 j_2) J_{12}, n\nu I'; I\rangle, \quad (n \leq N-1) \\ &|[(j_1 j_2) J_{12}, (j_3 j_4) J_{34}] J_F, n\nu I'; I\rangle, \quad (n \leq N-2) \ . \end{aligned} \tag{14}$$

$|n\nu I\rangle$ denotes a state with n quadrupole phonons [n d bosons and $(N-n)$ s bosons in the IBA representation] coupled to angular momentum I. Additional quantum numbers needed to specify the state are denoted by ν. The notation for fermion states is self-explanatory.

III. SU(3) LIMIT—STRONG COUPLING

The study of high-spin states in even-even nuclei, and especially the description of "backbending" phenomena[11] should present a straightforward application of the proposed model. In order to investigate the formation of band patterns based on two- and four-quasiparticle states in deformed nuclei, we consider a somewhat schematic case: a prolate boson core characterized by SU(3) symmetry and the fermion space restricted to the unique parity orbital $h_{\frac{11}{2}}$.

The boson part of the Hamiltonian (1) takes the form

$$H_B = -\frac{\alpha}{10} Q_2^B \cdot Q_2^B + \frac{\beta}{10} I_1^B \cdot I_1^B \ , \tag{15}$$

where the quadrupole operator is defined in Eq. (7), and I_1^B is the angular momentum operator

$$I_{1\mu}^B = \sqrt{10}(b_2^\dagger \tilde{b}_2)_{1\mu} \ . \tag{16}$$

The creation of a fermion pair out of the boson space breaks the SU(3) symmetry of the boson core (N decreases by one in the basis). The interaction between fermions will be dominated by long-range quadrupole forces that act through polarization of the core. The basic structure of the energy spectrum will be determined by the dynamical and mixing interactions. The residual fermion interaction and the exchange interaction will act as perturbation.

For a given type of boson core (prolate or oblate), the structure of two-quasiparticle bands depends basically on the position of the Fermi level. In odd-even nuclei (single fermion coupled to a boson core), a strongly coupled band pattern arises if a particle-type ($v_j^2 < 0.5$) fermion is coupled to an oblate core, or a hole-type ($v_j^2 > 0.5$) fermion to a prolate core. If on the other hand a particle-type fermion is coupled to a prolate core, or a hole-type fermion to an oblate core, the boson-fermion interaction is repulsive and a decoupled band pattern is formed. This rule can also be stated in terms of quadrupole moments.[12] The spectroscopic quadrupole moment of the boson core $Q_c(2_1) < 0$ for a prolate core, and $Q_c(2_1) > 0$ for an oblate core. For the odd-quasiparticle we have

$$\mathrm{sgn}[Q_{\mathrm{qp}}(\tilde{j})] = \mathrm{sgn}(2v_j^2 - 1) \ ,$$

and, therefore, for

$$Q_{\mathrm{qp}}(\tilde{j}) \cdot Q_c(2_1) \begin{cases} < 0, \text{ the band pattern is of a strongly coupled type} \\ > 0, \text{ the band pattern is decoupled} \ . \end{cases}$$

For the two-quasiparticle state $|(\tilde{j})^2 J\rangle$, the sign of the quadrupole moment is determined by

$$\mathrm{sgn}\{Q_{\mathrm{qp}}[(\tilde{j})^2 J]\} = \mathrm{sgn}[Q_{\mathrm{qp}}(\tilde{j})] \cdot \mathrm{sgn}\{3[J(J+1)-1] - 4j(j+1)\} \ .$$

For high values of J, $Q_{\mathrm{qp}}[(\tilde{j})^2 J]$ has the same sign as $Q_{\mathrm{qp}}(\tilde{j})$. As we shall see in the following, two-quasiparticle bands near the yrast line are dominated by high fermion angular momentum couplings. Therefore, for these states the same strongly-coupled/decoupled band pattern rule applies as for the case of a single quasiparticle coupled to a boson core.

In Fig. 1(a) we present the energy spectrum that is obtained by diagonalization of the Hamiltonian (1) in the basis (14) for the following set of parameters: prolate SU(3) core with $N=7$, $\alpha = 0.4$ MeV, $\beta = -0.05$ MeV; $h_{\frac{11}{2}}$ orbital with $v_{11/2}^2 = 0.8$ and $E_{11/2} = 1$ MeV; dynamical boson-fermion interaction with $\Gamma_0 = 0.32$ MeV and $\chi = -\sqrt{7}/2$. There is no mixing between states with different number of fermions. The two-body fermion interaction in Eq. (2), and the exchange interaction (9) are not included. Here we have hole-type fermions coupled to a prolate core, so that the spectrum presents a strongly coupled truncated band pattern. The equivalent situation in the geometrical model of Bohr and Mottelson[13] arises for the case of strong coupling of fermions to the deformation.

In order to keep the dimensions of bases under 10^3, a relatively small number of bosons, $N=7$, is included in all our calculations. Nevertheless, two- and four-quasiparticle rotational bands are well developed. For $\chi = -\sqrt{7}/2$, the boson part of the dynamical interaction is an SU(3) generator so that the Hamiltonian we have used does not mix states based on different SU(3) representations of the boson core. Therefore, the two- and four-quasiparticle bands that are shown in Fig. 1(a) are based on the ground-state band of the core. As we mentioned before, there is a small breaking of SU(3)-boson symmetry in two- and four-quasiparticle states. Nevertheless, we expect that the wave functions of the few lowest two-quasiparticle bands are, apart from Coriolis effects, described to a good approximation by the K-representation basis that was introduced in Refs. 14 and 15 for the description of rotational bands in deformed odd-odd nuclei. The KR-basis states are defined by

$$|(K_1,K_2)KJM\rangle = N \sum_{J_{12},I_c} \frac{1}{B_{I_c}} \langle J_{12} K I_c 0 | JK\rangle \langle j_1 K_1 j_2 K_2 | J_{12} K\rangle |(j_1 j_2) J_{12}, I_c; JM\rangle_{\mathrm{TWC}} \tag{17}$$

where N is the normalization constant and B_{I_c} is given by Eqs. (51), (52), and (54) of Ref. 10. The functions $1/B_{I_c}$ are also displayed in Fig. 1 of Ref. 15. The truncated weak-coupling (TWC) basis states are defined as

$$|(j_1 j_2) J_{12}, I_c; JM\rangle_{\mathrm{TWC}} = \sum_{m_{12},M_c} \langle J_{12} m_{12} I_c M_c | JM\rangle |(j_1 j_2) J_{12} m_{12}\rangle |I_c M_c\rangle \tag{18}$$

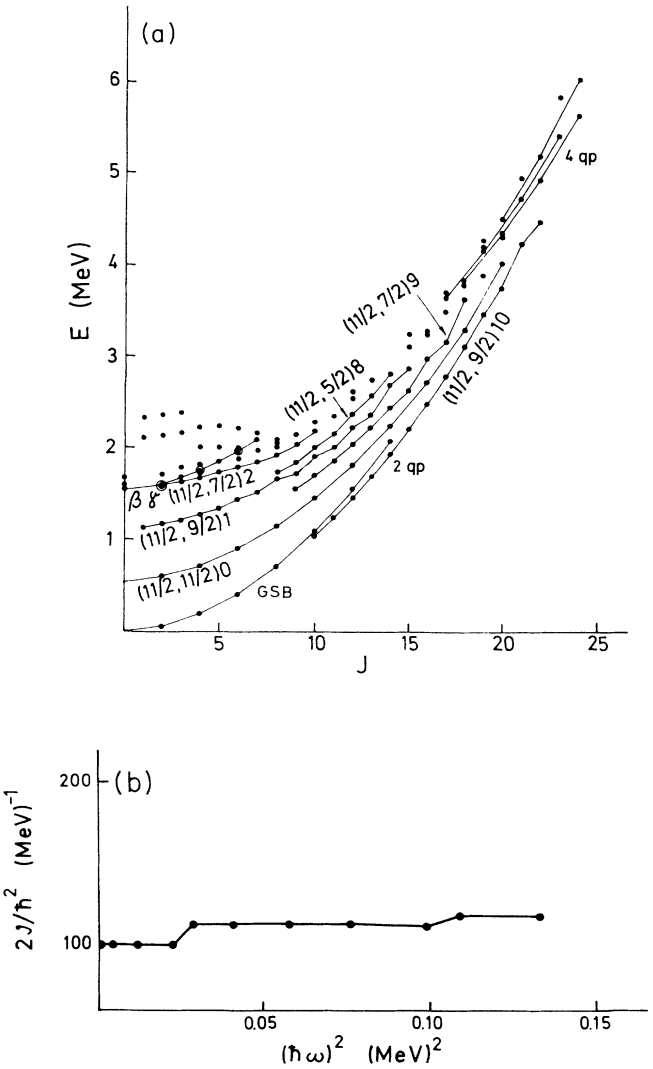

FIG. 1. (a) Excitation energy versus angular momentum for the illustrative IBA+2qp+4qp calculation: prolate SU(3) boson core with $N=7$, $h_{\frac{11}{2}}$ orbital with $v^2_{11/2}=0.8$ and $E_{11/2}=1$ MeV. Only the dynamical boson-fermion interaction is included with $\Gamma_0=0.32$ MeV, and there is no mixing between states with different number of fermions. For a description of the band pattern, see the text. (b) The moment of inertia as a function of angular velocity for the yrast states with even spin in (a). $2\mathcal{J}/\hbar^2$ and $\hbar\omega$ are calculated from Eqs. (20) and (21), respectively.

Here, $|(j_1j_2)J_{12}m_{12}\rangle$ denotes the two-quasiparticle state (in our example $j_1=j_2=\frac{11}{2}$). $|I_cM_c\rangle$ is the wave function of the state with angular momentum I_c and z projection M_c, which belongs to the ground-state band of the boson core.

The KR-basis (17) is derived by angular momentum projection from the adiabatic product of single-fermion intrinsic states and the SU(3) boson coherent state. $K_{1(2)}$ can be interpreted as the projection of $j_{1(2)}$ along the intrinsic symmetry axis, and J is the total angular momentum with projections K and M along the intrinsic symmetry and laboratory z axis, respectively. The K-representation basis represents the algebraic analog of the strong-coupling basis of the geometrical model.[13]

Comparing K-representation basis states to the wave functions that are obtained by diagonalization of the model Hamiltonian, we have grouped the lowest two-quasiparticle states in Fig. 1(a) in rotational bands characterized by "algebraic projections" $(K_1,K_2)K$ ($K=K_1+K_2$ or $|K_1-K_2|$). In order to make such a comparison, the wave functions of two-quasiparticle states based on the ground-state band of the core are transformed from the basis (14) into the TWC-basis (18):

$$\xi^{\mathrm{TWC}}_{J_{12},I_c}=\left[\sum_{n,\nu}(\eta_{J_{12},n\nu I_c})^2\right]^{1/2}$$

where $\eta_{J_{12},n\nu I_c}$ denotes amplitudes in the standard basis (14). Only amplitudes with an absolute value greater than 0.1 were taken into account. Since the KR-basis (17) is not orthogonal, one should also perform the Gram-Schmidt orthogonalization procedure in order of increasing energy when comparing it with wave functions that are obtained by diagonalization.

In Table I we present the KR-basis states for $(K_1=\frac{11}{2}, K_2=\frac{9}{2})$ $K=10$ and $N=6$. The wave functions of yrast states with $J\geq 10$ from Fig. 1(a) are shown in Table II (only amplitudes with an absolute value greater than 0.1). It is seen that these functions agree quite well for lower spins. Note that since $K=10$, the only nonvanishing components in the wave functions are those with the fermion coupling $J_{12}=10$. With increasing spin Coriolis effects become more pronounced. Besides the mixing with $(K_1=\frac{11}{2}, K_2=\frac{7}{2})K=9$, the yrast states have also small admixtures of states with $K=7,8$. Above $J=18$, Coriolis effects, now combined with strong truncation effects, make the identification of bands very difficult.

TABLE I. KR-basis states (17) for $(K_1=\frac{11}{2},K_2=\frac{9}{2})K=10$, expressed in the TWC basis (18).

		$\lvert J\rangle$								
J_{12}	I_c	10	11	12	13	14	15	16	17	18
10	0	0.41								
10	2	0.71	0.51	0.21						
10	4	0.52	0.69	0.63	0.42	0.19				
10	6	0.24	0.47	0.65	0.71	0.62	0.42	0.20		
10	8	0.07	0.19	0.35	0.53	0.68	0.73	0.67	0.50	0.27
10	10	0.01	0.04	0.10	0.21	0.35	0.51	0.66	0.77	0.77
10	12			0.02	0.04	0.08	0.15	0.26	0.41	0.58

TABLE II. Wave functions of the yrast states with $J \geq 10$ in Fig. 1(a), expressed in the TWC basis (18).

		$\lvert J_r\rangle$								
J_{12}	I_c	10_1	11_1	12_1	13_1	14_1	15_1	16_1	17_1	18_1
10	0	0.43								
10	2	0.73	0.56	0.21						
10	4	0.47	0.69	0.69	0.50	0.22				
10	6	0.15	0.40	0.61	0.73	0.71	0.58	0.35		
10	8			0.26	0.43	0.59	0.73	0.77	0.58	0.11
10	10					0.23	0.36	0.50	0.71	0.82
10	12							0.13	0.38	0.48

The wave functions in this region feel more strongly the breaking of the SU(3) boson symmetry. In Table III we compare the bandheads $(\frac{11}{2},\frac{11}{2})00$, $(\frac{11}{2},\frac{9}{2})11$, and $(\frac{11}{2},\frac{7}{2})99$ with the corresponding wave functions that are obtained by diagonalization. As seen from Fig. 1(a), the lowest two-quasiparticle bands are those with the highest values of K_1 and K_2. Of two bands having the same K_1 and K_2, the lower is the one with $K=K_1+K_2$. The wave functions of states that belong to the band $(K_1=\frac{11}{2},K_2=\frac{9}{2})K=1$ contain also components with low fermion angular momentum couplings. According to our previous discussion, such states tend to decouple from the boson core. The result is the odd-even staggering shown in Fig. 1(a). It is also interesting to notice the presence of the low-lying band $(K_1=\frac{11}{2},K_2=\frac{11}{2})K=0$. From Eq. (17) one can see that, for $j_1=j_2$, a band with $K=0$ contains only states with even values of the total angular momentum. Since most of the neighboring bands have high values of the quantum number K, the amount of admixtures in the band $(\frac{11}{2},\frac{11}{2})0$ is rather low. This also means that, with the inclusion of the mixing interaction (11), two-quasiparticle admixtures in the ground-state band come principally from the band $(\frac{11}{2},\frac{11}{2})0$.

TABLE III. Comparison of the KR-basis bandheads $(\frac{11}{2},\frac{11}{2})00$, $(\frac{11}{2},\frac{9}{2})11$, and $(\frac{11}{2},\frac{7}{2})99$, with the wave functions of the corresponding states in Fig. 1(a). The wave functions are expressed in the TWC basis (18).

J_{12}	I_c	$(K_1,K_2)KJ$	$\lvert J_r\rangle$
		$(\frac{11}{2},\frac{11}{2})00$	O_2
0	0	0.49	0.46
2	2	0.75	0.75
4	4	0.43	0.43
6	6	0.12	
8	8	0.02	
10	10		
		$(\frac{11}{2},\frac{9}{2})11$	1_1
2	2	−0.67	0.63
4	4	−0.69	0.69
6	6	−0.29	0.31
8	8	−0.05	
10	10		
		$(\frac{11}{2},\frac{7}{2})99$	9_1
10	2	−0.53	0.61
10	4	−0.70	0.67
10	6	−0.45	0.34
10	8	−0.16	
10	10	−0.03	

In Table IV the wave functions of the lowest four-quasiparticle states in Fig. 1(a) are expressed in the truncated weak-coupling basis

$$|(h\tfrac{11}{2})^4 J_F, I_c; J\rangle \ , \tag{19}$$

where $|I_c\rangle$ denotes the state with spin I_c that belongs to the ground-state band of the boson core.

In Fig. 1(b) we plot the moment of inertia $\mathcal{J}$ as a function of ω^2 for the yrast states with even spin. The moment of inertia is defined as

$$\frac{2\mathcal{J}}{\hbar^2}=\frac{2(2J-1)}{E(J)-E(J-2)} \ , \tag{20}$$

and the angular velocity is calculated from

$$\hbar\omega=\frac{E(J)-E(J-2)}{\sqrt{J(J+1)}-\sqrt{(J-2)(J-1)}} \ . \tag{21}$$

Since the boson core is characterized by SU(3) symmetry, the moment of inertia is constant in the ground-state band. At $J=10$ the two-quasiparticle band $(\frac{11}{2},\frac{9}{2})10$ becomes the yrast-band, and there is a sharp increase of the moment of inertia. The value of $\mathcal{J}$ in this band is some 12% higher than in the ground-state band, and remains nearly constant up to $J=18$ where Coriolis and truncation effects cause a further increase. The increase of $\mathcal{J}$ at $J=10$ is not accompanied by a decrease in ω^2, so what we have here is really an "upbending" of $\mathcal{J}$ as a function of ω^2.

In the next step we have investigated the effect of the mixing interaction (11) on the yrast states. Figure 2(a) presents the energy spectrum that is obtained by diagonalization of the model Hamiltonian for the same set of parameters as the one shown in Fig. 1(a), except that now the mixing interaction is also included with the strength parameter $\varepsilon_0=0.2$ MeV. This value has been chosen in

order to obtain a crossing between the ground-state band and the two-quasiparticle band $(\frac{11}{2},\frac{9}{2})10$ near the $J=12$ yrast state. The mixing interaction (11) contains a fermion operator of rank 2, so that states that belong to the ground-state band can be connected in the first order to two-quasiparticle basis states with fermion coupling $J_{12}=2$. As is seen from Eq. (17), states that belong to a band $(K_1,K_2)K$ based on the ground-state band of the core cannot have fermion couplings with $J_{12}<K$. Therefore, the ground-state band mainly interacts with the two-quasiparticle bands $(\frac{11}{2},\frac{11}{2})0$ and $(\frac{11}{2},\frac{9}{2})1$. The result is an increase of the moment of inertia of the ground-state band. As we shall see, the mixing interaction has practically no effect on the band $(\frac{11}{2},\frac{9}{2})10$, and therefore the bending of the ground-state band causes its crossing with $(\frac{11}{2},\frac{9}{2})10$. Since the mixing (11) is the only block off-diagonal interaction we have used, the behavior of the energy spectrum does not depend on the sign of the interaction. The amount of admixtures in the ground-state band is 9% for the ground state $|0_1\rangle$, and increases very slowly to 10% for $|10_1\rangle$. These admixtures are mainly states based on two quasiparticles with $J_{12}=2$. The amount of four-quasiparticle admixtures in the ground-state band is below 1%. The interaction also breaks to some extent the SU(3) symmetry in the boson part (0 fermions) of the wave functions. In order to enhance the

TABLE IV. Wave functions of the lowest high-spin four-quasiparticle states in Fig. 1(a), expressed in the TWC basis (19).

$\|J_r\rangle$	$\|(h\frac{11}{2})^4 J_F, I_c\rangle$
18_5	$0.32\|(h\frac{11}{2})^4 10,8_c\rangle$
	$-0.18\|(h\frac{11}{2})^4 11,8_c\rangle$
	$0.56\|(h\frac{11}{2})^4 12,6_c\rangle$
	$-0.21\|(h\frac{11}{2})^4 13,6_c\rangle$
	$0.56\|(h\frac{11}{2})^4 14,4_c\rangle$
	$0.33\|(h\frac{11}{2})^4 16,2_c\rangle$
19_3	$-0.21\|(h\frac{11}{2})^4 12,8_c\rangle$
	$-0.40\|(h\frac{11}{2})^4 14,6_c\rangle$
	$-0.67\|(h\frac{11}{2})^4 16,4_c\rangle$
	$-0.47\|(h\frac{11}{2})^4 16,6_c\rangle$
	$-0.22\|(h\frac{11}{2})^4 16,8_c\rangle$
20_4	$0.16\|(h\frac{11}{2})^4 10,10_c\rangle$
	$0.45\|(h\frac{11}{2})^4 12,8_c\rangle$
	$-0.16\|(h\frac{11}{2})^4 13,8_c\rangle$
	$0.66\|(h\frac{11}{2})^4 14,6_c\rangle$
	$0.51\|(h\frac{11}{2})^4 16,4_c\rangle$
21_2	$-0.15\|(h\frac{11}{2})^4 12,10_c\rangle$
	$0.11\|(h\frac{11}{2})^4 13,8_c\rangle$
	$-0.46\|(h\frac{11}{2})^4 14,8_c\rangle$
	$-0.78\|(h\frac{11}{2})^4 16,6_c\rangle$
	$-0.34\|(h\frac{11}{2})^4 16,8_c\rangle$
22_2	$0.27\|(h\frac{11}{2})^4 12,10_c\rangle$
	$0.63\|(h\frac{11}{2})^4 14,8_c\rangle$
	$0.70\|(h\frac{11}{2})^4 16,6_c\rangle$
	$0.12\|(h\frac{11}{2})^4 16,8_c\rangle$
23_1	$0.37\|(h\frac{11}{2})^4 14,10_c\rangle$
	$0.89\|(h\frac{11}{2})^4 16,8_c\rangle$
	$0.24\|(h\frac{11}{2})^4 16,10_c\rangle$
24_1	$0.50\|(h\frac{11}{2})^4 14,10_c\rangle$
	$0.85\|(h\frac{11}{2})^4 16,8_c\rangle$
	$0.14\|(h\frac{11}{2})^4 16,10_c\rangle$

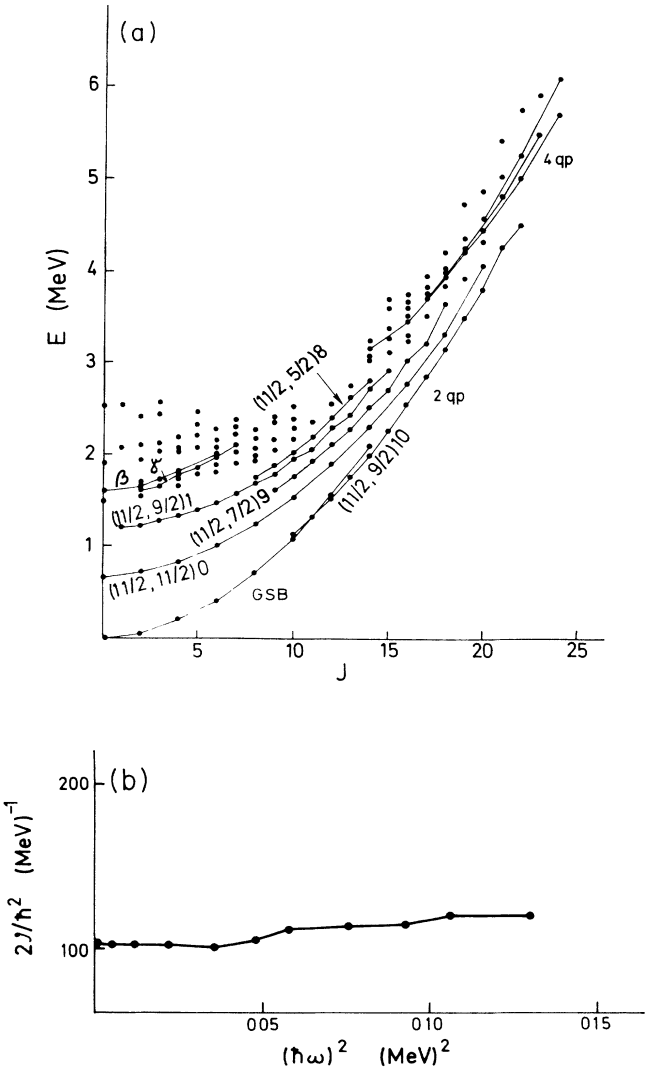

FIG. 2. (a) The energy spectrum that is calculated for the same set of parameters as the one shown in Fig. 1(a), except that now the mixing interaction (11) is included with $\varepsilon_0=0.2$ MeV. (b) The plot of $\mathcal{J}$ vs ω^2 for the yrast states in Fig. 2(a).

mixing with two-quasiparticle states for higher-spin members of the ground-state band, one could add interactions that contain fermion operators of higher rank, i.e., 4,6,. . . . However, such an interaction would also imply higher order boson matrix elements, so that its overall contribution could be rather small. The yrast states after the crossing, i.e., states that belong to the $(\frac{11}{2},\frac{9}{2})10$ band, are practically unaffected by the mixing interaction (11). Since the dominant components have fermion coupling $J_{12}=10$, the mixing interaction cannot connect these states directly to zero-fermion states. The mixing with four-quasiparticle states becomes visible only for higher spins, $J \geq 16$. However, the amount of four-quasiparticle admixtures does not exceed 5%.

In Fig. 2(b) we plot $\mathcal{J}$ vs ω^2 for the yrast states with even spin from Fig. 2(a). As compared to the case without mixing interaction [Fig. 1(b)], the moment of inertia of the ground-state band is higher by $\approx 2\%$, and the increase of $\mathcal{J}$ to the value it has in the band $(\frac{11}{2},\frac{9}{2})10$ is now more smooth. Thus, we have obtained a crossing of the ground-state band with the lowest two-quasiparticle band, which is not accompanied with a backbending of the moment of inertia. We can say that the behavior of $\mathcal{J}$ vs ω^2 is determined by the interaction of the ground-state band with two-quasiparticle states, but not with the band it crosses.

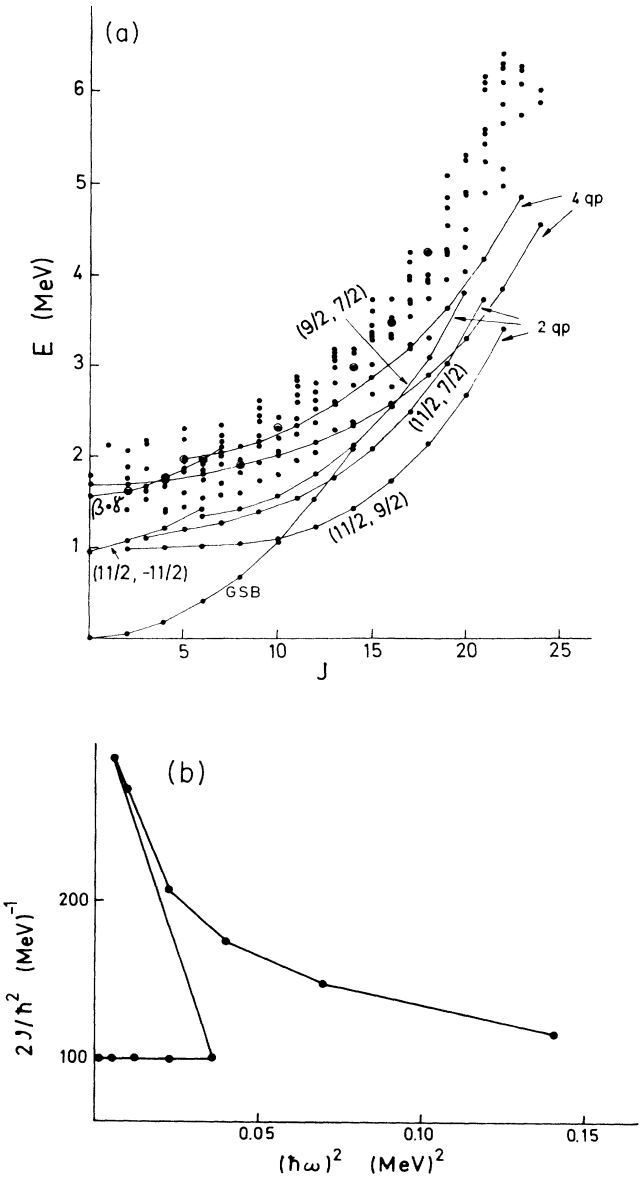

FIG. 3. (a) Decoupled band pattern in the illustrative IBA+2qp+4qp calculation: prolate SU(3) boson core with $N=7$, $h\frac{11}{2}$ orbital with $v^2_{11/2}=0.2$ and $E_{11/2}=1$ MeV, and the dynamical boson-fermion interaction with $\Gamma_0=0.4$ MeV. (b) $\mathcal{J}$ vs ω^2 for yrast states in (a).

IV. SU(3) LIMIT—DECOUPLING

In this section we investigate the spectrum that arises in coupling particle-type fermions to an SU(3) prolate core or, equivalently, hole-type fermions to an oblate core. This case corresponds in the geometrical model to the situation in which fermions are decoupled from the deformation and, under the action of the Coriolis force, tend to align their angular momenta along the axis of rotation.[16,17]

The energy spectrum shown in Fig. 3(a) presents the result of diagonalization of the Hamiltonian (1) for the same set of parameters as in our first example from Sec. III, except that $v^2_{11/2}$ has been changed from 0.8 to 0.2. Again, only the dynamical part of the boson-fermion interaction is included with $\Gamma_0=0.4$ MeV. There is no mixing between states with different fermion number. Two-quasiparticle states are organized into decoupled rotational bands with $\Delta J=2$ between neighboring states. These bands do not have sharp bandheads, i.e., the projections of angular momenta on the symmetry axis are not good quantum numbers. The only exact quantum number with which these bands can be characterized is the signature:[13] $r=+1$ (-1) for states with even (odd) spin. The splitting between states with different signature can also be noted in the lowest lying four-quasiparticle states.

In analogy to the treatment of decoupled structure in odd-even nuclei in the framework of the IBFM,[18] we introduce a new algebraic basis for the description of two-quasiparticle states

$$|(\alpha_1,\alpha_2)JM\rangle = N \sum_{K_1,K_2} \langle 2N\,0\,j_1K_1|2N+\alpha_1K_1\rangle \times \langle 2N\,0\,j_2K_2|2N+\alpha_2K_2\rangle \times |(K_1,K_2)K_1+K_2JM\rangle \quad (22)$$

On the right-hand side we use nonorthogonal KR-basis vectors (17), and the sum runs over both positive and negative values of K_1 and K_2. In the geometrical limit, when the boson number $N\rightarrow\infty$, one has[19]

$$\lim_{2N\rightarrow\infty} \langle 2N\,0\,jK|2N+\alpha K\rangle = d^j_{K\alpha}(\pi/2)\ . \quad (23)$$

Therefore, Eq. (22) represents the algebraic analog of the strong-coupling–to–rotation-aligned transformation of Stephens.[17] The quantum numbers α_1 and α_2 correspond

to the projections of fermion angular momenta j_1 and j_2 on the rotational axis. As for the KR basis, the states (22) are orthogonalized in order of increasing energy. For two-quasiparticle states in the geometrical model, one also has a more specific definition of the signature quantum number. Namely,

$$\mathcal{R}_1|(\alpha_1,\alpha_2)JM\rangle=(-)^{J-(\alpha_1+\alpha_2)}|(\alpha_1,\alpha_2)JM\rangle \quad (24)$$

where $\mathcal{R}_1=e^{i\pi I_1}$ is the rotation operator, and I_1 is the body-fixed component of the collective angular momentum of the core. Therefore, in order that the wave functions fulfill the $\mathcal{R}_1$ symmetry (rotation of the core by π around the 1 axis), $J-(\alpha_1+\alpha_2)$ has to be even. Bands characterized by (α_1,α_2) contain only even-spin or only odd-spin states.

Comparing the wave functions that are obtained by di-

TABLE V. Comparison of the decoupling-basis states (22) for $(\alpha_1,\alpha_2)=(\frac{11}{2},\frac{9}{2})$ and $(\frac{11}{2},\frac{7}{2})$, with the wave functions of the corresponding states in Fig. 3(a). The wave functions are expressed in the TWC basis (18).

J_{12}	I_c	$(\alpha_1,\alpha_2)J$	$\|J_r\rangle$	J_{12}	I_c	$(\alpha_1,\alpha_2)J$	$\|J_r\rangle$
		$(\frac{11}{2},\frac{9}{2})10$	10_2	8	6	−0.12	0.44
6	4		0.30	8	8		−0.18
8	2	0.18	−0.48	10	4	−0.94	−0.62
8	4		0.19	10	6	0.31	0.49
10	0	0.80	0.49	10	8		−0.23
10	2	−0.54	−0.42				
10	4	0.17	0.24			$(\frac{11}{2},\frac{7}{2})15$	15_1
				8	8	−0.10	0.38
		$(\frac{11}{2},\frac{9}{2})12$	12_1	10	6	−0.98	−0.77
6	6		0.20	10	8	0.19	0.42
8	4	0.15	−0.46	10	10		−0.12
10	2	0.94	0.71				
10	4	−0.29	−0.37			$(\frac{11}{2},\frac{7}{2})17$	17_1
10	6		0.10	8	10		0.21
				10	8	−0.99	−0.90
		$(\frac{11}{2},\frac{9}{2})14$	14_1	10	10	0.11	0.36
8	6	0.13	−0.41				
10	4	0.98	0.80			$(\frac{11}{2},-\frac{11}{2})0$	0_2
10	6	−0.18	−0.32	0	0	0.74	0.64
				2	2	−0.60	−0.61
		$(\frac{11}{2},\frac{9}{2})16$	16_1	4	4	0.29	0.39
8	8	0.11	−0.34	6	6		−0.16
10	6	0.99	0.88				
10	8	−0.11	−0.26			$(\frac{11}{2},-\frac{11}{2})2$	2_3
				0	2	0.46	0.17
		$(\frac{11}{2},\frac{9}{2})18$	18_1	2	0	0.24	0.45
8	10		−0.17	2	2	0.77	0.67
10	8	0.99	0.95	2	4	−0.11	
10	10		−0.22	4	2		−0.16
				4	4	−0.34	−0.40
		$(\frac{11}{2},\frac{7}{2})11$	11_1	6	6		0.16
6	6		−0.29				
8	4	−0.15	0.44			$(\frac{11}{2},-\frac{11}{2})4$	4_3
8	6		−0.29	0	4	0.40	0.39
10	2	−0.83	−0.39	2	4	0.70	0.67
10	4	0.52	0.47	4	0		−0.16
10	6	−0.14	−0.33	4	2	0.27	
				4	4	0.47	0.26
		$(\frac{11}{2},\frac{7}{2})13$	13_1	4	6	−0.13	−0.27
6	8		−0.18	6	6	−0.14	

agonalization of the model Hamiltonian to the basis (22), we have assigned the algebraic quantum numbers (α_1,α_2) to the lowest-lying two-quasiparticle bands in Fig. 3(a). The lowest-lying states are the ones that are maximally aligned $(\alpha_1=j,\alpha_2=j-1)$. This corresponds to the picture of unpaired fermions whose angular momenta are oriented perpendicular to the symmetry axis, while the core is completely decoupled and rotates with $I=J-(\alpha_1+\alpha_2)$. The second lowest band has $(\alpha_1=\frac{11}{2},\alpha_2=\frac{7}{2})$ and consists of odd-spin states. We have also identified a third band as $(\alpha_1=\frac{9}{2},\alpha_2=\frac{7}{2})$. Because of strong Coriolis mixing, it is rather hard to classify higher states in bands described by the simple basis (22). For the two lowest bands $(\frac{11}{2},\frac{9}{2})$ and $(\frac{11}{2},\frac{7}{2})$, we compare in Table V the wave functions of some high-spin states with the corresponding algebraic functions (22). The wave functions are expressed in the truncated weak-coupling basis (18), and only amplitudes with an absolute value greater than 0.1 are shown. First, we notice that with increasing spin the algebraic basis (22) becomes a better approximation to the exact wave functions. This is in accordance with similar investigations in the geometrical model.[17] The algebraic functions do not include mixing effects, and therefore they are more "aligned" than the wave functions that are obtained by diagonalization. That means that the component with

$$J_{12}=2j-1\equiv(J_{12})_{\max} \quad \text{and} \quad I_c=J-(2j-1)$$

will be more pronounced in the algebraic basis. The band $(\frac{11}{2},\frac{9}{2})$ is based mainly on $J_{12}=2j-1=10$, and the main components in the band $(\frac{9}{2},\frac{7}{2})$ are those with $J_{12}=8$. As is seen from Table V, the mixing between these bands gives a higher amplitude for the $J_{12}=8$ components of $(\frac{11}{2},\frac{9}{2})$, and also a difference in phase, as compared to pure algebraic functions. In accordance with results that are obtained in the geometrical model,[17] it is found that the algebraic basis (22) is appropriate for the description of states with $J\geq 2j-1$. For states with lower spin, the only quantum number that remains is the signature. However, from Fig. 3(a) it seems that there is at least one exception: the band $(\frac{11}{2},-\frac{11}{2})$. States in which one of the fermion angular momenta is oriented antiparallel to the angular momentum of the core, are generally expected at a somewhat higher excitation energy. For low spins, i.e., in the absence of rotation, a state $(\alpha_1,-\alpha_2)J$ will be only slightly above $(\alpha_1,\alpha_2)J$. Because of large projections on the rotational axis, the band $(\frac{11}{2},-\frac{11}{2})$ lies exceptionally low in energy in the low-spin part of the spectrum. On the other hand, since α_2 is negative, these states do not mix very much with their neighbors. Therefore we have been able, by comparing with the algebraic basis (22), to identify several low-spin members of $(\frac{11}{2},-\frac{11}{2})$. For the first three states the comparison is shown in Table V. It is interesting to note that the band $(\frac{11}{2},-\frac{11}{2})$ is behaving much in the same way as the $(\frac{11}{2},\frac{11}{2})0$ band in the strong-coupling limit [Fig. 1(a)].

If the lowest high-spin four-quasiparticle states from Fig. 3(a) are expressed in the TWC basis (19), it is seen that the wave functions are very similar to those that were obtained in the strong-coupling limit and that are displayed in Table IV. However, in the present case the alignment in the wave functions of even-spin states is somewhat more pronounced. The components with $J_F\equiv(J_F)_{\max}=16$ and $I_c=J-(J_F)_{\max}$ have higher amplitudes (by $\approx 15\%$) than in the strong-coupling limit. For states with lower spin, the distribution of amplitudes over fermion angular momenta is gradually shifted towards lower values of J_F. In the standard basis (14), the amplitudes are fragmented over hundreds of components, making the interpretation of the wave functions very difficult.

In Fig. 3(b) the moment of inertia as a function of the angular velocity is shown for the yrast states up to $J=22$. As is seen from Fig. 3(a), the crossing between

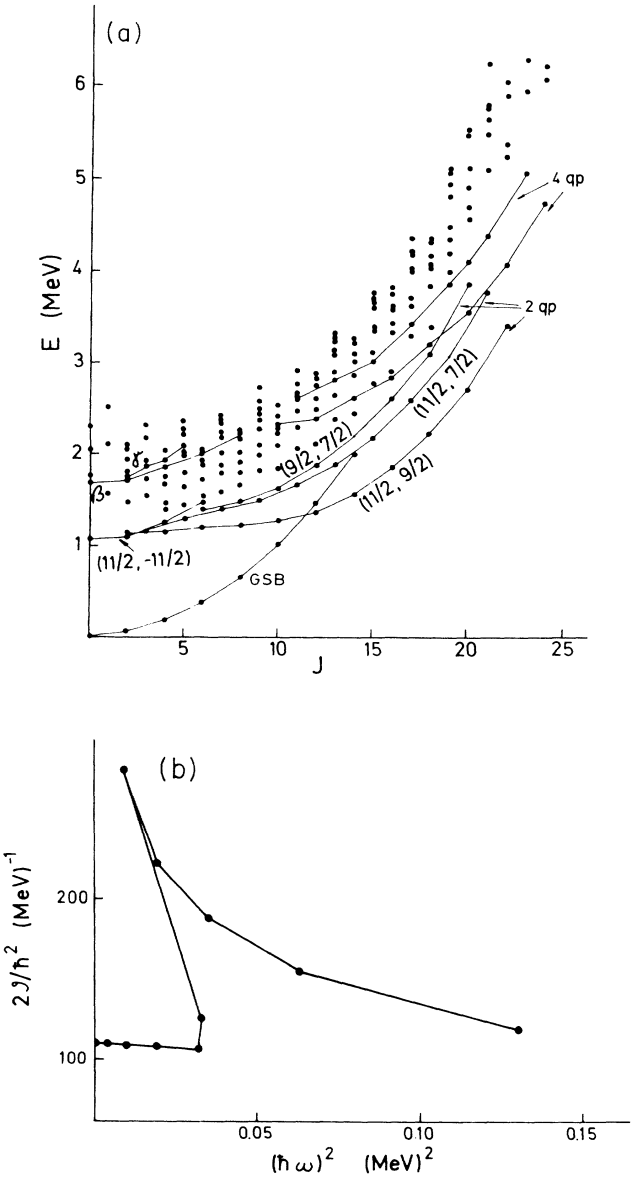

FIG. 4. (a) The energy spectrum that is calculated for the same strength parameters as the one shown in Fig. 3(a), and with the inclusion of the mixing interaction (11) with $\varepsilon_0=0.5$ MeV. (b) $\mathcal{J}$ vs ω^2 for the yrast states in (a).

the ground-state band and the two-quasiparticle band $(\frac{11}{2},\frac{9}{2})$ lies in the region where the latter is almost flat with energy. The backbending of the moment of inertia is very pronounced. Immediately after the intersection, the value of $\mathcal{J}$ is nearly three times that of the ground-state band (somewhat lower, for lower values of Γ_0). With increasing spin, the moment of inertia decreases very rapidly to a value that is somewhat higher than that of the ground-state band. Although the numerical values depend on the strength of the dynamical interaction, the plot of $\mathcal{J}$ vs ω^2 looks very much the same for all values of Γ_0 for which there is an intersection between the two bands. We note that a very similar behavior of the moment of inertia has been obtained in the framework of the geometrical model.[16]

The effects of the mixing interaction (11) are shown in Fig. 4(a). The calculation is performed for the same set of parameters as the one shown in Fig. 3(a), and the mixing interaction is included with the strength parameter $\varepsilon_0=0.5$ MeV. The mixing with two- and four-quasiparticle states results in an increase of the moment of inertia of the ground-state band. Because of the bending of the ground-state band, the point of intersection with the two-quasiparticle band $(\frac{11}{2},\frac{9}{2})$ is shifted toward $J=12$. We also notice a higher density of states compared to the spectrum that is obtained without the mixing interaction. The strong mixing makes rather difficult the identification of four-quasiparticle states; especially in the low-spin region. With the inclusion of the mixing interaction the β and γ bands are no longer degenerate. However, as compared to the strong-coupling limit [see Fig. 2(a)], it is interesting to note that the degeneracy is removed in a different way. In the present case the γ band lies above the β band.

TABLE VI. The wave functions of yrast states that belong to the ground-state band in Fig. 4(a). Two-quasiparticle states are expressed in the TWC basis (18). The percentage of two- and four-quasiparticle admixtures is given in the third column; the percentage of four-quasiparticle admixtures is given separately in the last column.

$\|J_r\rangle$		2qp+4qp	4qp
0_1	$0.93\|0_c\rangle$	14%	3%
	$0.17\|(h\frac{11}{2})^2 0,0_c\rangle$		
	$-0.30\|(h\frac{11}{2})^2 2,2_c\rangle$		
2_1	$0.93\|2_c\rangle$	14%	3%
	$0.14\|(h\frac{11}{2})^2 0,2_c\rangle$		
	$-0.17\|(h\frac{11}{2})^2 2,0_c\rangle$		
	$0.15\|(h\frac{11}{2})^2 2,2_c\rangle$		
	$-0.15\|(h\frac{11}{2})^2 2,4_c\rangle$		
4_1	$0.92\|4_c\rangle$	15%	3%
	$0.14\|(h\frac{11}{2})^2 0,4_c\rangle$		
	$-0.21\|(h\frac{11}{2})^2 2,2_c\rangle$		
	$0.12\|(h\frac{11}{2})^2 2,4_c\rangle$		
6_1	$0.91\|6_c\rangle$	17%	4%
	$0.13\|(h\frac{11}{2})^2 0,6_c\rangle$		
	$-0.27\|(h\frac{11}{2})^2 2,4_c\rangle$		
	$0.13\|(h\frac{11}{2})^2 2,6_c\rangle$		
8_1	$0.91\|8_c\rangle$	18%	4%
	$0.13\|(h\frac{11}{2})^2 0,8_c\rangle$		
	$-0.32\|(h\frac{11}{2})^2 2,6_c\rangle$		
	$0.11\|(h\frac{11}{2})^2 2,8_c\rangle$		
10_1	$0.89\|10_c\rangle$	20%	5%
	$0.11\|(h\frac{11}{2})^2 0,10_c\rangle$		
	$-0.35\|(h\frac{11}{2})^2 2,8_c\rangle$		
	$0.13\|(h\frac{11}{2})^2 4,6_c\rangle$		

In Table VI we present the wave functions of yrast states that belong to the ground-state band in Fig. 4(a). Only amplitudes with an absolute value greater than 0.1 are shown. As before, $|I_c\rangle$ denotes the collective state that belongs to the ground-state band, and two-quasiparticle states are expressed in the TWC basis (18). The percentage of two- and four-quasiparticle admixtures in these wave functions is given in the third column. It is seen that the amount of admixtures increases slowly along the yrast line. Finally, in the fourth column of Table VI we give separately the percentage of four-quasiparticle states in the yrast wave functions. From the structure of the wave functions that are displayed in Table V, it is clear that the mixing interaction will have little effect on the yrast states that belong to the band $(\frac{11}{2},\frac{9}{2})$. There is practically no mixing with collective states (also because there are no collective states above $J=14$), and the mixing with four-quasiparticle states becomes significant only above $J=16$. The amount of four-quasiparticle admixtures is somewhere around 10%.

The plot of the moment of inertia for the yrast states is shown in Fig. 4(b). Compared to the case without mixing [Fig. 3(b)], the value of $\mathcal{J}$ in the ground-state band is higher by $\approx 10\%$. The moment of inertia immediately after the intersection is somewhat lower, but the overall effect of the mixing interaction in the region of band crossing is very small.

V. CONCLUSIONS

In this work we have investigated the SU(3) limit of the IBA model extended with two- and four-quasiparticle excitations. This model should provide a description of rotational bands based on two- and four-quasiparticle states in deformed even-even nuclei. First, we have shown that, for low-lying two-quasiparticle bands, the same strongly coupled/decoupled band pattern rule applies as for the case of a single quasiparticle coupled to the boson core. For hole-type (particle-type) fermions coupled to the SU(3) prolate (oblate) core, the product $Q_c(2_1)\cdot Q_{qp}[(\tilde{j})^2 J]<0$, and the resulting band pattern is of a strongly-coupled type. The low-lying two-quasiparticle bands are described by the algebraic K-

representation basis that was recently introduced in the interacting boson-fermion-fermion model for the description of rotational bands in odd-odd nuclei. This basis is the algebraic analog of the strong-coupling basis of the geometrical model. Therefore, it provides a geometrical interpretation of the wave functions that are obtained by diagonalization of the model Hamiltonian. With the inclusion of an interaction that mixes states with different number of fermions in the model Hamiltonian, we have obtained a crossing of the ground-state band with the lowest two-quasiparticle band. This crossing, however, is not accompanied by a backbending of the moment of inertia. In fact, we have shown that the behavior of the moment of inertia in the region of band crossing is determined by the interaction of the ground-state band with two-quasiparticle states, but not with the band it crosses.

In the case of particle-type (hole-type) fermions coupled to the SU(3) prolate (oblate) core, the boson-fermion interaction for the low-lying two-quasiparticle bands is repulsive, and a decoupled band pattern arises. The four-quasiparticle bands are rather low in energy, compared to the strong-coupling limit. By an algebraic transformation of the K-representation basis, we have derived a new decoupling-basis that provides a good approximation for the low-lying two-quasiparticle bands. In the limit of large boson number, this basis becomes equivalent to the strong-coupling–to–rotation-aligned transformation of Stephens. Therefore, the lowest two-quasiparticle bands can be characterized by "algebraic projections" of fermion angular momenta on the axis of rotation. The crossing of the ground-state band with the most aligned two-quasiparticle band gives an extremely strong backbending of the moment of inertia as a function of angular velocity. Although the mixing interaction we have used changes the structure of the wave functions of the yrast states, its effect on the moment of inertia in the region of band crossing is very small. In order to obtain a greater effect, one should probably use mixing interactions that contain fermion operators of higher rank. Of special interest is also the inclusion of a larger number of bosons in the calculation. In that case one would be able to attempt a description of the second backbending in the crossing with a four-quasiparticle band. We note that since all calculations in the present approach are performed in the laboratory frame, the results can be directly compared with the experimental data, in contrast to the cranking model calculations.[11] Moreover, the model is suitable for description of two- and four-quasiparticle states in transitional and O(6)-like nuclei where the cranking model cannot be applied.

ACKNOWLEDGMENTS

This work was partially supported by the Italian Ministry of Public Education and Istituto Nazionale di Fisica Nucleare.

[1]A. Arima and F. Iachello, Phys. Rev. Lett. **35**, 1069 (1975); F. Iachello and A. Arima, *The Interacting Boson Model* (Cambridge University Press, Cambridge, 1987).

[2]A. Gelberg and A. Zemel, Phys. Rev. C **22**, 937 (1980); N. Yoshida, A. Arima, and T. Otsuka, Phys. Lett. **114B**, 86 (1982).

[3]C. E. Alonso, J. M. Arias, and M. Lozano, Phys. Lett. B **177**, 130 (1986).

[4]I. Morrison, A. Faessler, and C. Lima, Nucl. Phys. **A372**, 13 (1981); A. Faessler, S. Kuyucak, A. Petrovici, and L. Petersen, Nucl. Phys. **A438**, 78 (1985).

[5]D. S. Chuu and S. T. Hsieh, Phys. Rev. C **38**, 960 (1988); D. S. Chuu, S. T. Hsieh, and H. C. Chiang, Phys. Rev. C **40**, 382 (1989).

[6]J. P. Elliot, Rep. Prog. Phys. **48**, 171 (1985).

[7]D. Janssen, R. V. Jolos, and F. Dönau, Nucl. Phys. **A224**, 93 (1974).

[8]K. Allaart, E. Boeker, G. Bonsignori, M. Savoia, and Y. K. Gambhir, Phys. Rep. **169**, 209 (1988).

[9]F. Iachello and O. Scholten, Phys. Rev. Lett. **43**, 679 (1979).

[10]V. Paar, S. Brant, L. F. Canto, G. Leander, and M. Vouk, Nucl. Phys. **A378**, 41 (1982).

[11]M. J. A. de Voigt, J. Dudek, and Z. Szymanski, Rev. Mod. Phys. **55**, 949 (1983).

[12]G. Alaga and V. Paar, Phys. Lett. **61B**, 129 (1976).

[13]A. Bohr and B. R. Mottelson, *Nuclear Structure* (Benjamin, New York, 1975).

[14]S. Brant, V. Paar, D. K. Sunko, and D. Vretenar, Phys. Rev. C **37**, 830 (1988).

[15]D. Vretenar, S. Brant, V. Paar, and D. K. Sunko, Phys. Rev. C **41**, 757 (1990).

[16]F. S. Stephens and R. S. Simon, Nucl. Phys. **A183**, 257 (1972).

[17]F. S. Stephens, Rev. Mod. Phys. **47**, 43 (1975).

[18]D. K. Sunko and V. Paar, Phys. Lett. **146B**, 279 (1984).

[19]L. C. Biedenharn and J. D. Louck, *Angular Momentum in Quantum Physics* (Addison-Wesley, New York, 1981).